92-16468

# REPORT DOCUMENTATION PAGE

Form Approved OMB No. 0704-0188

| 1. AGENCY USE ONLY (Leave blank) | 2. REPORT DATE<br>May 1992 | 3. REPORT TYPE AND DATES COVERED |
|---|---|---|

**4. TITLE AND SUBTITLE**
DESIGN MODIFICATION AND CALIBRATION OF THE PICATIINNY ACTIVATOR FOR SETBACK SAFETY TESTING OF SADARM

**5. FUNDING NUMBERS**

**6. AUTHOR(S)**
Barry Fishburn

**7. PERFORMING ORGANIZATION NAME(S) AND ADDRESSES(S)**
ARDEC, AED
Energetics and Warheads Division (SMCAR -AEE-WW)
Picatinny Arsenal, NJ 07806-5000

**8. PERFORMING ORGANIZATION REPORT NUMBER**
Technical Report ARAED-TR-92001

**9. SPONSORING/MONITORING AGENCY NAME(S) AND ADDRESS(S)**
ARDEC, IMD
STINFO Br (SMCAR-IMI-I)
Picatinny Arsenal, NJ 07806-5000

**10. SPONSORING/MONITORING AGENCY REPORT NUMBER**

**11. SUPPLEMENTARY NOTES**

**12a. DISTRIBUTION/AVAILABILITY STATEMENT**

Approved for public release; distribution is unlimited.

**12b. DISTRIBUTION CODE**

**13. ABSTRACT (Maximum 200 words)**
The relationship between conditions in the Picatinny activator setback testing machine and conditions during an artillery launch of a projectile having a base gap is elucidated through computer simulation of both events. The testing machine simulation is used to prescribe a much improved design for the device, which can then come close to duplicating the launch conditions. The previous design produced overly high pressures and very lengthy pulse durations compared to what is expected during a launch. It also suffered from vibrations which adversely affected repeatability of results. The new design eliminates these problems and can be used to simulate launches even at accelerations high compared to typical artillery launches.

**14. SUBJECT TERMS**
Artillery          Premature
Activator test     Base gap
Shell

**15. NUMBER OF PAGES**
36

**16. PRICE CODE**

| 17. SECURITY CLASSIFICATION OF REPORT | 18. SECURITY CLASSIFICATION OF THIS PAGE | 19. SECURITY CLASSIFICATION OF ABSTRACT | 20. LIMITATION OF ABSTRACT |
|---|---|---|---|
| UNCLASSIFIED | UNCLASSIFIED | UNCLASSIFIED | SAR |

# CONTENTS

i

## TABLES

## FIGURES

# INTRODUCTION

There are several testing machines around the world which have been used to simulate the effects of a gun launch on explosive warheads with a base gap (refs 1,2,3,4,5). We restrict to planar air gaps as opposed to cavities in the explosive material. There has been limited analysis of the relationship between the test conditions produced in these machines and actual conditions during launches . This study was undertaken to allow calibration of the Picatinny activator setback testing machine so that a given test condition can be related to a particular launch condition.

The activator is basically a one-dimensional device. Thus it seems appropriate to consider a one-dimensional model of the launch as well. It can be argued that this represents a worse case situation in the sense that planar gaps are as sensitive in the activator as the most sensitive case of cavities in the explosive (at least for Comp B). However, it has been shown in the past that hemispherical cavities in a soft material placed in contact with an explosive (like Sylgard rubber or even water) can be very small (radius less than the minimum gap), and still produce ignition, primarily due to convergence effects. We neglect this case.

## LAUNCH CONDITIONS

The one-dimensional model used to represent launch conditions is shown in figure 1. Above the liner, there is a free surface. This will generally be the case in artillery shells, as the steel walls move before the fill because of their stiffness. The air gap is treated as having uniform conditions while the fill is treated as undergoing elastic-perfectly plastic plane strain (no lateral expansion allowed) (ref 6). Material properties for the elastic-perfectly plastic model were estimated from high rate triaxial compression tests on Composition B carried out at ARDEC as well as assorted handbook values. Because of the interplay between rate of loading and elastic constants for explosives, the model used should only be considered as representative of a generic explosive filler, sufficient for elucidating the physics of base gap closure. Following previous work, we postulate a worse case as being an instantaneously acquired, steady acceleration of the piston representing the shell base. The calculated pressure in the air generated by this boundary condition when the fill column height is 9.7 cm is shown in figure 2 (a and b).

The first rise in air pressure, to $P_1$, occurs very fast, within 1 or 2 microseconds. This is rapid enough that a weak shock wave is sent up through the fill. Thus the compressibility of the fill is important. In fact, the change in length of the explosive is fairly large compared to the size of the gap when it has achieved maximum compression. With the shock propagating up the fill column, the pressure in the air continues to rise until $P_2$ is obtained, but at a vastly slower rate. This steady rise continues until the expansion from the top of the fill arrives back at the air gap about 100 microseconds later. As seen in figure 2b, several such pulses will occur, although, arguably the first is most severe. Finally, the correct hydrostatic pressure distribution (linearly increasing pressure towards the base) is obtained after 1.2 milliseconds. The air temperature, computed from

1

$$q = \frac{6.8\, k\left[T_{air} - T_{fill}\right]}{\Delta x_{air}}$$

with conductivity given by

$$k = 0.0242 \left(\frac{T}{273.16}\right)^{0.8} \frac{watts}{meter\ {}^{o}K}$$

and $\qquad\qquad \Delta x_{air}$ = instantaneous gap width

which has been used by a previous author is shown in figure 3. Losses to the shell were accounted for by doubling the heat transfer to the fill. This attempts to address the case where an insulative layer is on the shell wall whose thermal properties are similar to that of the fill. A coarse approach to describing heat transfer is necessitated by the fact that temperature gradients occur on a length scale quite small compared to the scale required to describe the dynamics of gap closure. The sophistication of this simulation, which is intended to follow the dynamics of gap closure, can not simultaneously treat the temperature gradients. Thus, accurate prediction of explosive temperatures is not possible and only the average temperature pulse in the air is obtained. Because the heat transfer is taken as inversely proportional to the instantaneous gap width, it becomes very large when the gap is fully compressed. Peak temperature is associated with the initial pressure jump and decays significantly even while the pressure is still rising towards $P_2$. Only the initial jump produces anything like an adiabatic compression, and even this jump is not fast enough for truly adiabatic temperatures to be obtained. It is clear that the rate of pressure rise associated with the first jump is crucial to the temperatures which can be obtained. The value of $P_2$, by contrast, has little to do with temperature.

Initial pulses always have the form indicated in figure 2a. The small excursion near the end of this pulse is due to reflection from a heavy liner riding atop the explosive. Its duration is too short to affect things very much. Variations in $P_1$ and $P_2$ with gap size for 20 KG's and 30 KG's acceleration, and for the 20 KG's case with the heat transfer arbitrarily reduced to 10% of its regular value is shown in figure 4. The ordinate scale is pressure divided by the appropriate hydrostatic pressure. Higher acceleration does not give as large a loading factor as lower accelerations, although the absolute pressures are higher. In general, variation with gap size is different from variation with acceleration, but each has a comparable effect on pressure over this range of gap sizes. The duration of the pressure pulse for all these calculations is nominally 100 microseconds, which is set by the length of the fill column, and is independent of anything else. That is, the duration is determined by the time required

for a (sonic) compression wave to return from the top of the fill as an expansion. This time is nominally twice the column length divided by the filler sound speed.

The peak temperatures corresponding to the calculations in figure 4 are shown in figure 5. Between 2/3 mm and 1 mm gap sizes, changes in gap size have a comparable effect as do changes in acceleration; however, below 2/3 mm gaps, peak temperature is much more sensitive to gap size than to acceleration. The curve with 10% heat transfer begins to plateau beyond 1 mm gaps, indicative of the adiabatic compression temperature having nearly been obtained for larger gaps with slow heat transfer.

The half height width of the temperature pulses in microseconds is shown in figure 6. The calculated pulses, assuming regular heat transfer, are exceedingly short (of order 10 microseconds) and decrease with gap size. The slow heat transfer calculations have a much wider variation in pulse duration, exceeding 60 microseconds with 1 mm gaps.

Changing the heat transfer rate by a factor of 10 affects the calculated air temperatures dramatically, even though the pressure histories are not greatly affected. However, even with the slower heat transfer, the peak temperature still coincides with the first pressure jump to $P_1$. The changes caused by assuming slower heat transfer is a larger peak temperature and a much more gradual rate of decay of temperature. Because of the dramatic effect of heat transfer on temperature, but secondary effect on pressure, a simulation of launch conditions needs to focus on reproducing the pressure pulse, since this will insure the heating effect is about correct. The proper heat transfer expression will always be in doubt, especially when a variety of fills is under consideration.

These calculations were based on a worse case scenario of constant acceleration, which implies that the mass of filler is vanishingly small compared to the mass of the shell. For the projectile under consideration here, ratio of charge mass to shell mass can be taken to 0.0715. If the constant acceleration assumption is replaced by a constant applied force to the shell mass (due to the applied gun pressure), only small changes in the air pressure pulse are generated. For example, with reference to the 20 KG's case (1 mm gap), $P_1$ would decrease by 3.5% and $P_2$ by 15%. Pulse duration would stay the same and the first temperature spike is indistinguishable from that obtained by assuming constant acceleration. When larger charge to mass ratios are considered, the constant acceleration assumption increasingly overestimates the conditions in the gap.

The pressure jump to $P_1$ occurs so fast that the change in shell velocity due to acceleration is negligible. In effect, the important part of the gap compression occurs with the relative velocity between the two sides of the gap kept nearly constant. So pressure rise rate depends strongly on the value of this closing velocity at first jump-up and its value is plotted in figure 7. It only depends on gap size and acceleration and appears to be the most important parameter associated with gap compression. Values

range between 10 and 25 M/S which sets the required piston velocity needed in any setback testing machine.

A summary of the important parameters associated with the first pressure rise is given in table 1. Any setback tester needs to be able to match these parameters.

## ACTIVATOR TESTING

The Picatinny activator is shown schematically in figure 8. The mass of the hammer (slightly over 2 kg) would require a driving pressure of $8.84 \times 10^{-2}$ GPa (12835 psi) to achieve an acceleration of 20 KG's. In order to operate at less pressure, the hammer section is made to impact a drift, which ultimately closes the gap. In this way the drift is shock accelerated, and effectively closes the gap with a high initial velocity. The hammer velocity is achieved using only $2.07 \times 10^{-3}$ GPa driving pressure, making operation simple with bottled compressed air. However, determining the stimulus level in the gap now becomes complex, and numerical simulation is required. The simulation treats the hammer and drift as made from 1.14 GPa yield steel undergoing plane stress. Any initial pressure distribution in the hammer, caused by its acceleration after the restraining shear pins break, has been neglected. Thus, the initial condition is the hammer, having zero pressure, but a given velocity (related to free run), in contact with the drift having zero velocity. A shock propagates from the contact, setting the drift in motion. Then the drift compresses the air gap against the sample, which is perfectly confined in a cup and modeled exactly the same as for the launch case. Heat transfer from the air is also treated the same as before. The end of the drift is assumed to have the same conductivity as the explosive (the end of the drift needs to be insulated for this to be true).

Results for a hammer velocity of 7 M/S driving a 1 mm air gap are shown in figure 9 (a through f). This simulation indicates that after the first reverberation of the shock through the drift, the drift velocity exceeds the hammer velocity although a considerable vibration is trapped in the drift. Then, as the drift slows due to compression of air in the gap, the trailing hammer, which has not yet lost much velocity, impacts it a second time, providing a large crushing effect on the sample. The pressure pulse in the air gap is shown in figure 9a. The peak pressure is greater than 0.9 GPa (130,000 psi) and the entire pulse lasts about 550 microseconds. The velocity of the gap end of the drift is displayed in figure 9b. An oscillation due to drift vibration is visible during the early drift motion. Then, after the second impact of the hammer, severe vibrations occur during the crushing. The compression stroke of the gap end of the drift is shown in figure 9c. The stroke is noticeably larger than the gap dimension and significant compression of the sample occurs. The computed temperature in the air is shown in figure 9d. High temperature occurs along with the first pressure rise, to about 0.037 GPa, then the air is cool over most of the compression stroke. A very small temperature rise occurs as a result of the second impact. The position of the surface of the sample during the stroke is shown in figure 9e. It is compressed almost 1 mm by the air pressure. Lastly, pressure on the back

4

wall of the sample confinement is shown in figure 9f. For all practical purposes, it is a carbon copy of the air pressure.

In this simulation, the end of the drift undergoes regular vibrations in velocity between 10.8 M/S and 14.7 M/S while it closes the gap. The rapid jump-up in pressure starts when the velocity is about 13 M/S. If the goal is to have the drift velocity match those given in table 1, thus coming close to creating nearly launch-like conditions, then the drift vibrations make this goal essentially impossible and add a random aspect to the experiment. That is, very small changes in the time at which the pressure jump-up occurs can cause it to happen at a significantly different velocity. Further, the maximum crushing effect on the sample has a pressure about seven times the maximum value achieved during a launch at 20 KG's for the column height under consideration. This is a rather severe over-pressure.

The drift velocity from the 7 M/S hammer is on the low side of closing velocities in table 1. Higher velocities are needed. A simulation with hammer speed of 14 M/S is shown in figures 10a through 10f for a 1 mm gap. Figure sequence corresponds to the previous usage. At this velocity, the yield strength of the steel is exceeded, causing the pressure pulse to have a flat-topped appearance. The gap end of the drift now oscillates between 18.4 M/S and 30.0 M/S, with the first pressure occurring when the velocity is 23.2 M/S and reaching 0.07 GPa. Peak temperature is about 1450 K, compared to only 1220 K for the 7 M/S case and 1480 K for the 30 KG's launch with 1 mm gap. The total explosive compression reached about 1.1 mm and, again, the back wall pressure is a carbon copy of the air pressure.

These results show the activator produces pressure pulses that are much larger than expected during launch. However, the critical first pressure rise can be made to mimic that in the launch by proper choice of hammer velocity and (as will be shown) drift length. However, it is vitally important that the huge crushing effect of the hammer on the totally confined sample be removed in order to have a similarity between events in the activator and those during launch.

A first attempt to remove the huge pressures in the activator, is to stop the hammer after it sets the drift in motion. Simulation with a 14 M/S hammer which is removed after the drift has moved 0.25 mm is shown in figures 11a through 11f. This is equivalent to having the drift barely protrude from a heavy, rigidly supported cylinder which is capable of stopping the hammer. The crushing effect of the hammer is thus removed; however, the drift is thrown back into the stopped hammer repeatedly. The air pressure is shown in figure 11a. Obviously, the pressure pulse is much smaller and shorter than before, lasting about 78 microseconds. The first pressure rise is to 7.0 GPa and occurs when the drift velocity is 18.7 M/S. However, the velocity of the end of the drift is undergoing a strong deceleration at that moment due to its vibration and so the first pressure rise appears softer than it needs to be if it is to replicate a launch. Peak temperature is affected by this vibration. Ultimately a maximum pressure of 45 GPa is obtained. The strong drift vibrations and pressures which are still too high show this alone cannot simulate launch conditions.

5

The vibrations in the drift can be eliminated by choosing the drift to be equal to or shorter than the hammer. Then the drift is fully accelerated to rigid body motion in one reverberation, and all vibrations are trapped in the hammer. Secondly, a direct method of controlling the duration of the pulse is to increase the length of the sample to actual size and have a free surface boundary condition opposite the air gap end. In addition, it helps to have as long a drift as practical. For the Picatinny activator, a 7.62 cm long drift was chosen. This configuration was modeled and a typical result is shown in figure 12a through 12e for a hammer speed of 14 M/S and 1 mm air gap. A clean first pressure rise to 0.091 GPa, followed by a triple terraced deceleration before the expansion from the sample free surface arrives at 130 microseconds is shown in figure 12a. The terraces result because deceleration of the drift occurs via wave motion passing back and forth within it (remember the hammer is no longer in contact with the rear of the drift when the drift closes the gap, so the rear has become a free surface boundary ). The closing velocity of the drift at the gap is shown in figure 12b. A uniform, constant velocity of 25.4 M/S is produced by the hammer impact which persists until the pressure jump-up occurs near 50 microseconds. The loss in gap end drift velocity at pressure jump-up is 2.57 M/S (10.1%). The drift end moves around 2 mm during the pressure pulse as shown in figure 12c and the calculated temperature spike associated with the pressure pulse, with a peak value of 1525 K and pulse width at half height of 8.46 microseconds is shown in figure 12d. The velocity of the surface of the sample, which is first accelerated by the air pressure and then by the reflected expansion from the free surface at the other end is shown in figure 12e. A large vibration is trapped in the sample.

A matrix of simulations was made for this new design and results are presented in figures 13 through 16. The drift closing velocity generated by a given hammer velocity is shown in figure 13. Over this range, the yield stress of the steel is not exceeded, so this line can be calculated without need of the computer simulation. The simulation can handle cases where the yield is exceeded, however. The manner in which $P_1$ depends on hammer velocity is shown in figure 14. The small difference displayed by the 1/3 mm gap is due to changes made to the simulation to suppress a numerical instability which appeared when the initial gap size became too small. The calculated peak air temperature is shown in figure 15 and the pulse width of the temperature spike is shown in figure 16. Calculated sample exit velocities for 1 mm gaps are shown in figure 17, and range upwards of 50 M/S. Provision for catching these samples is necessary. These curves constitute a calibration of the activator. For example, consider the 20 KG's launch with a 2/3 mm gap. Calculated conditions in the gap are given in table 2. Each parameter can be matched by the activator using a narrow band of hammer velocities as shown. Note that matching the closing velocity produces exactly the correct temperature; however, the $P_1$ pressure appears slightly low. As noted before, in the activator, the drift decelerates somewhat as the pressure jump-up occurs. By assumption, nothing like this can happen in the constant acceleration launch, since the motion of the left side of the gap is artifically imposed. Initial deceleration of the drift occurs because the steel shows some compressibility effects at these pressures. If the base of the shell in the constant acceleration calculation were endowed with compressible properties, undoubtedly some similar effect would occur. Probably, the best choice is to match $P_1$ in the activator with that in

6

the launch for a given gap. Thus, a hammer velocity of 10.3 M/S simulates a 20 KG's launch for a 2/3 mm gap based on this approach. In the case of very slow heat transfer, some allowance needs to be given to the fact that the activator pressure pulse rings down with a series of three terraces, whereas the launch pulse has a rising plateau characteristic. One can require the lowest of the terraces match the launch $P_2$ to ensure a conservative assessment of ignition criteria. An appropriate hammer velocity to achieve this can be chosen using the model.

## CONCLUSION

A one-dimensional, constant acceleration simulation of the launch of a short column height projectile with base gap has been exercised, and the important physics of the gap air compression determined. While the peak pressure depends on gap size and acceleration, as expected, it also depends strongly on the compressibility of the explosive fill, which had been previously pointed out in reference 7. The peak air temperature depends primarily on how rapidly the first pressure jump occurs, as this jump only requires a few microseconds. The value of pressure at the end of this first pressure jump does not depend on the column height of the explosive.

Computer modeling of the activator has surfaced some problems with the design that cause vibrations which affect test results. Suggestions for removing these problems have been introduced to the model and calculations completed which provide a means of relating activator free run to launch conditions. It is clear that the free run mode can provide gap conditions equivalent to launches even at very high accelerations. An exact duplication of the launch pressure time history, as calculated with the constant acceleration assumption, is not possible, but a very close approximation can be achieved. The modified design removes the great overpressures present in virtually all previous setback testers.

7

## Table 1. Computed conditions for launch

| Gap (mm) | Acceleration (KG's) | $P_1$ ($10^{-3}$MB) | $U_{closing}$ (M/S) |
|---|---|---|---|
| 1.00 | 20 | 0.80 | 20.0 |
|  | 30 | 0.97 | 24.0 |
| 0.67 | 20 | 0.64 | 16.1 |
|  | 30 | 0.79 | 20.0 |
| 0.33 | 20 | 0.49 | 11.2 |
|  | 30 | 0.56 | 14.4 |

## Table 2. Comparison of activator with launch

|  | $U_{closing}$ (M/S) | $U_{hammer}$ (M/S) | $P_1$ ($10^3$MB) | Tmax (K) | Duration (microsec) |
|---|---|---|---|---|---|
| 20 KG's Launch | 16.1 |  | 0.64 | 1243 | 10.7 |
| Activator | 16.1 | 9.0 | 0.552 | 1243 | 6.76 |
| Activator | 18.75 | 10.3 | 0.64 | 1300 | 8.08 |
| Activator | 12.9 | 7.13 | 0.431 | 1132 | 10.7 |
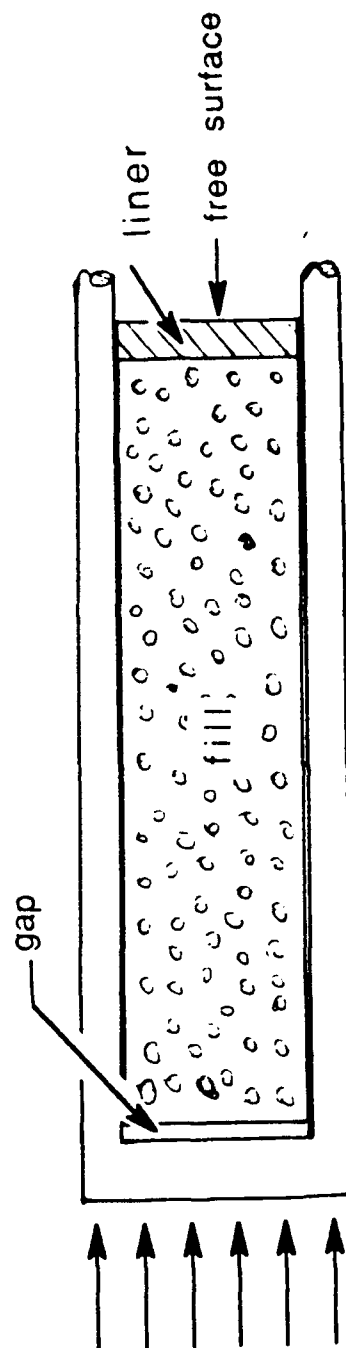
Figure 1. Constant acceleration launch model
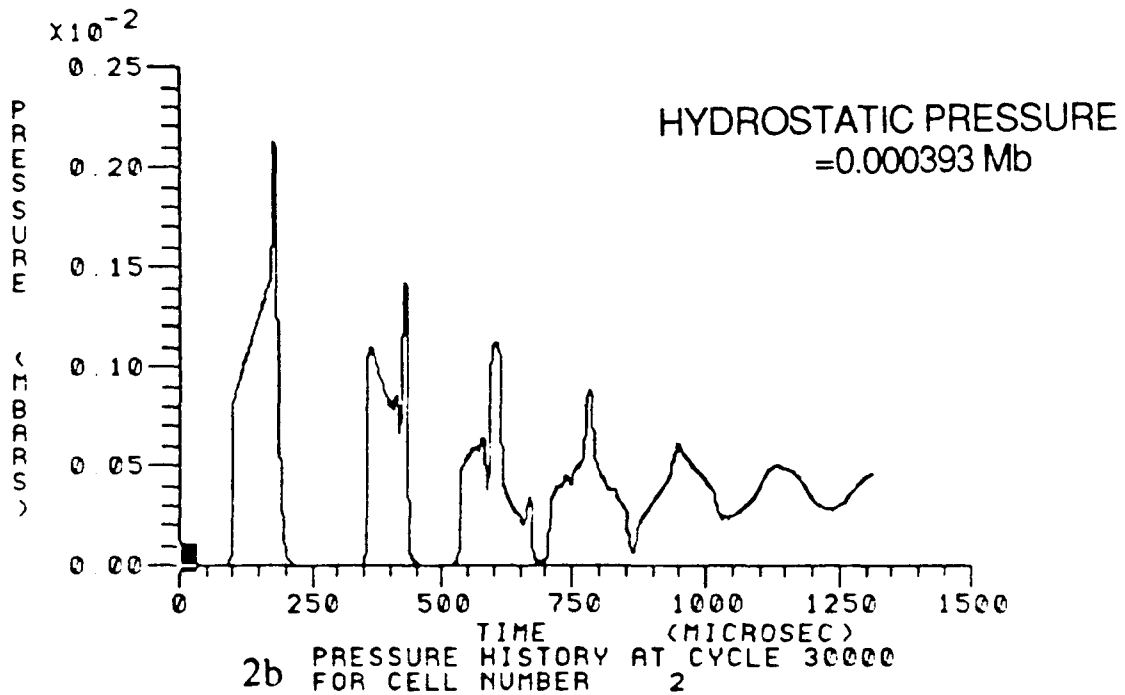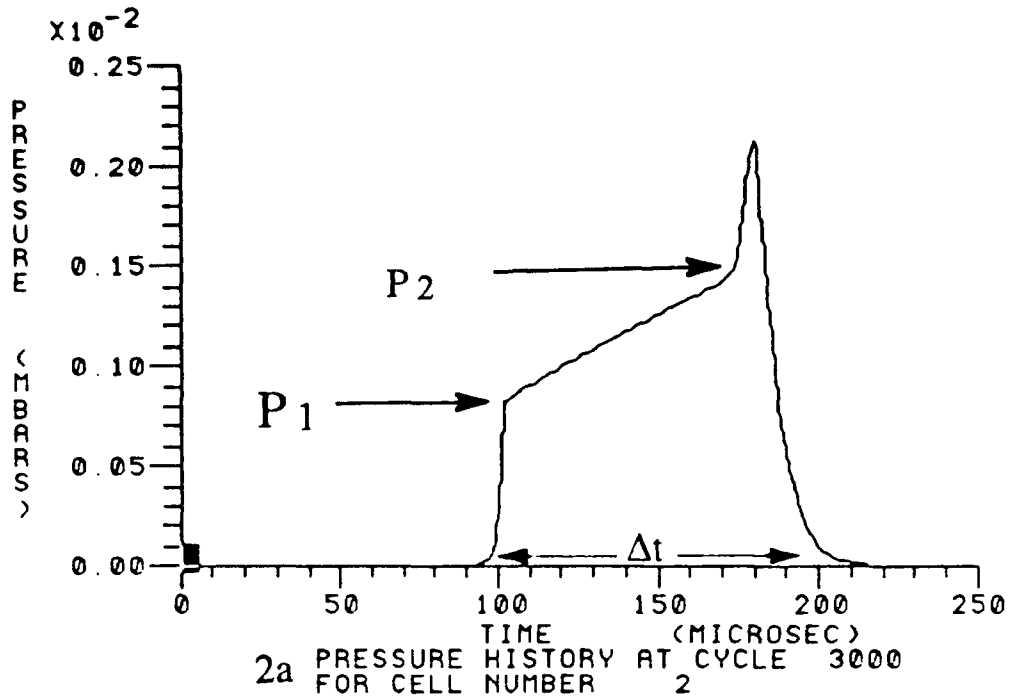
Figure 2. Launch air pressures
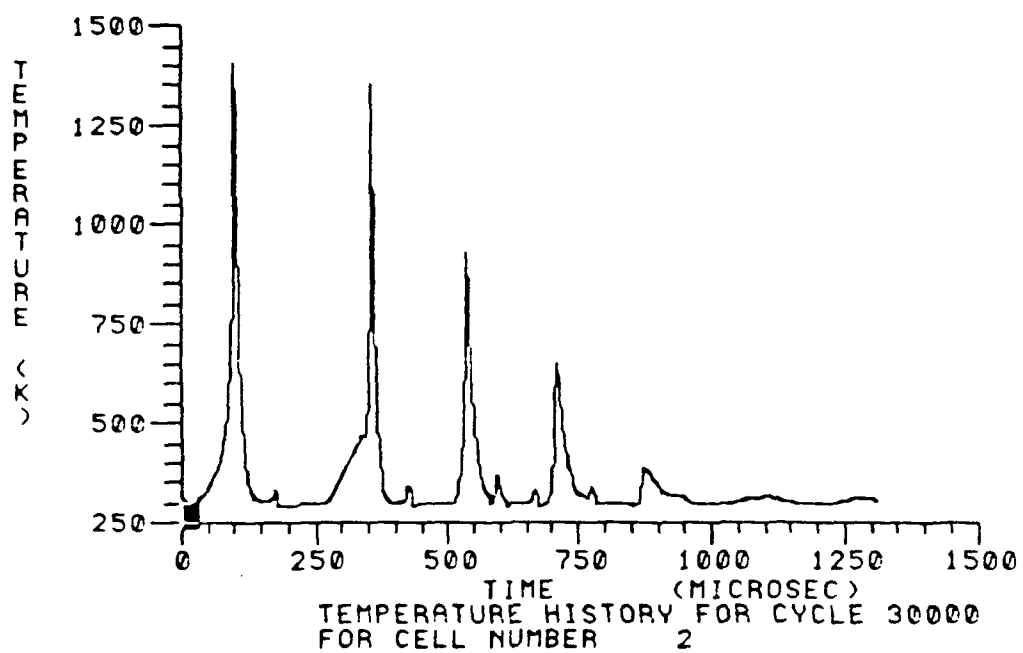
Figure 3. Launch air temperatures

13
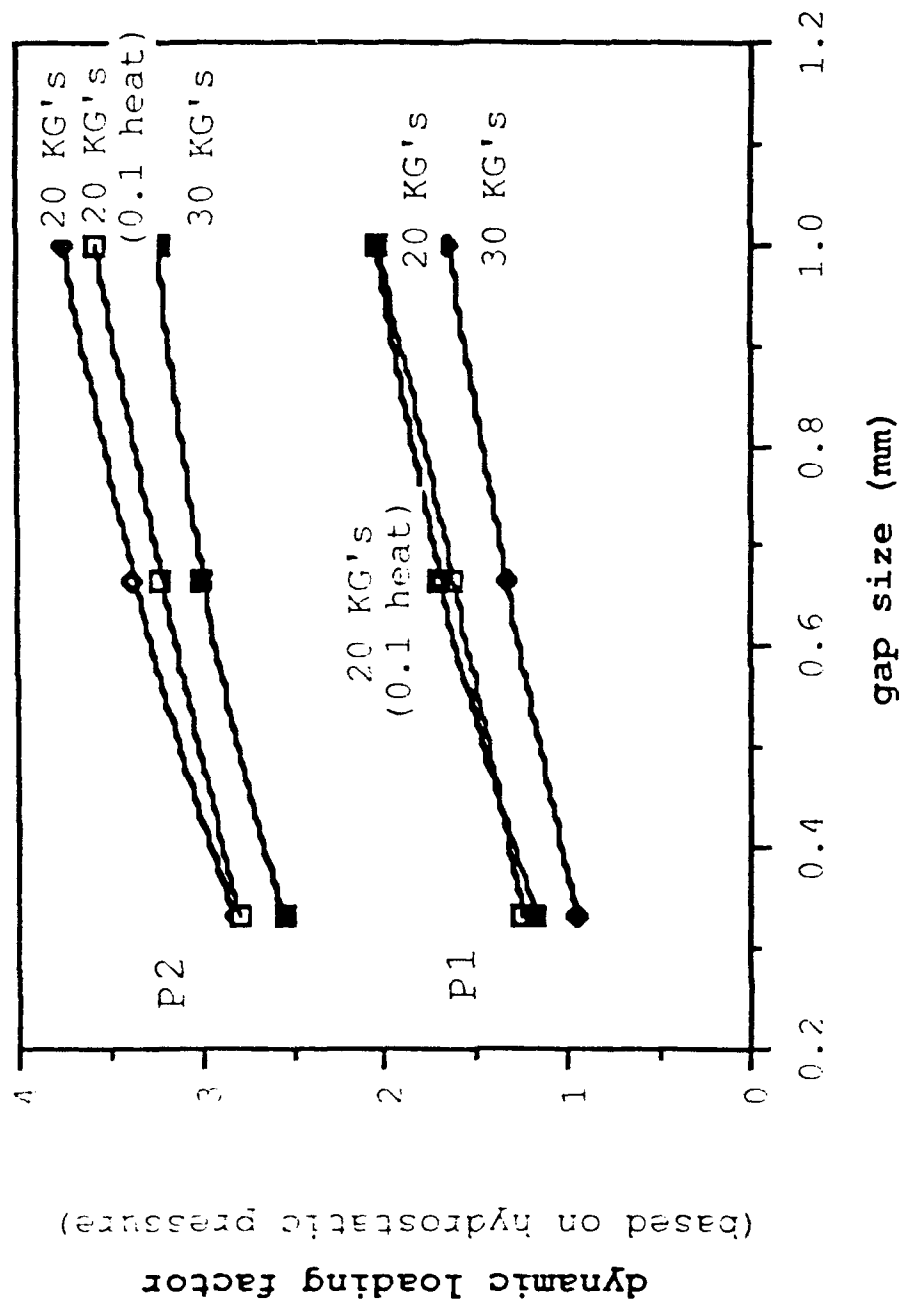
Figure 4. Launch peak air pressures
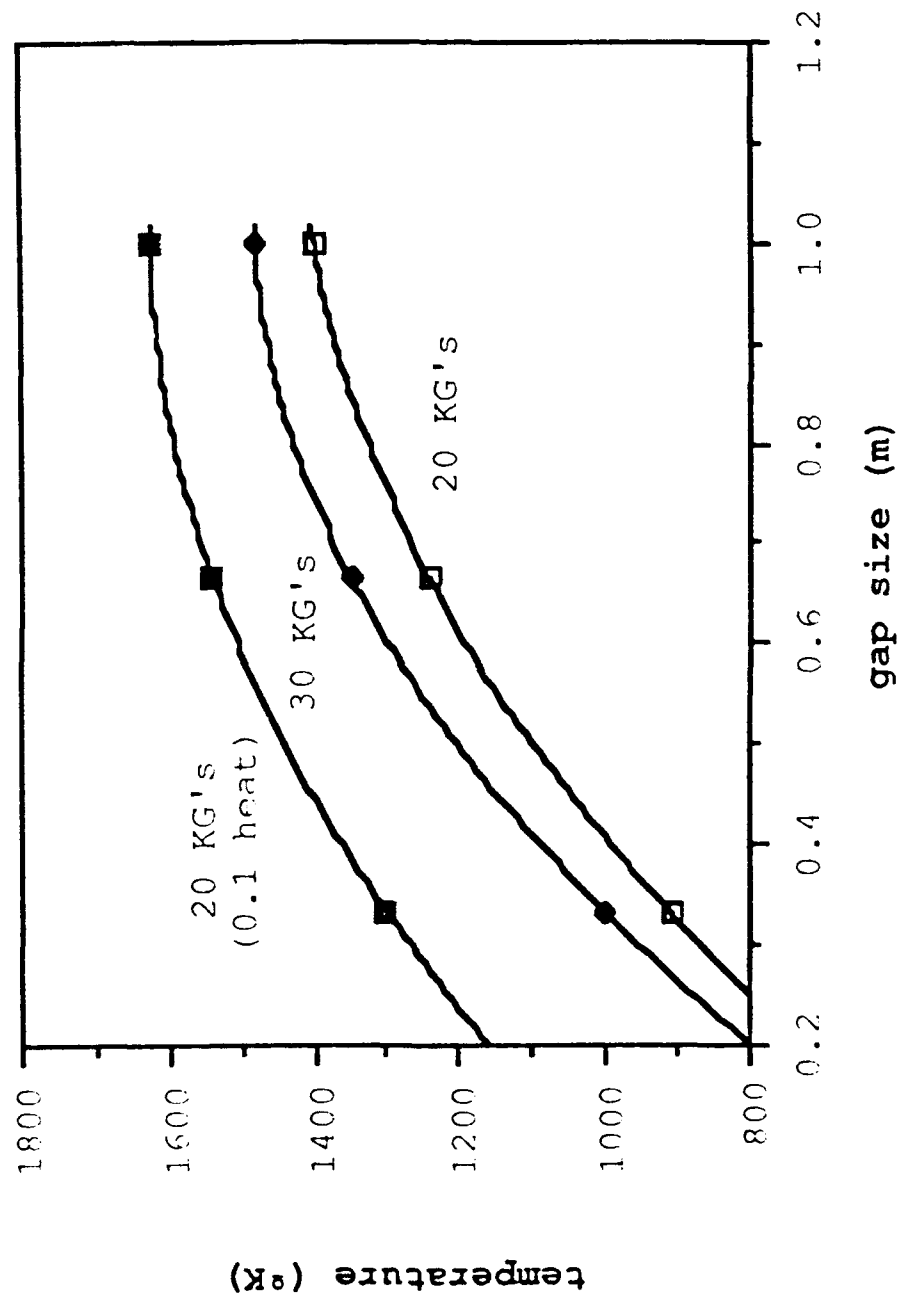
Figure 5. Launch peak air temperatures
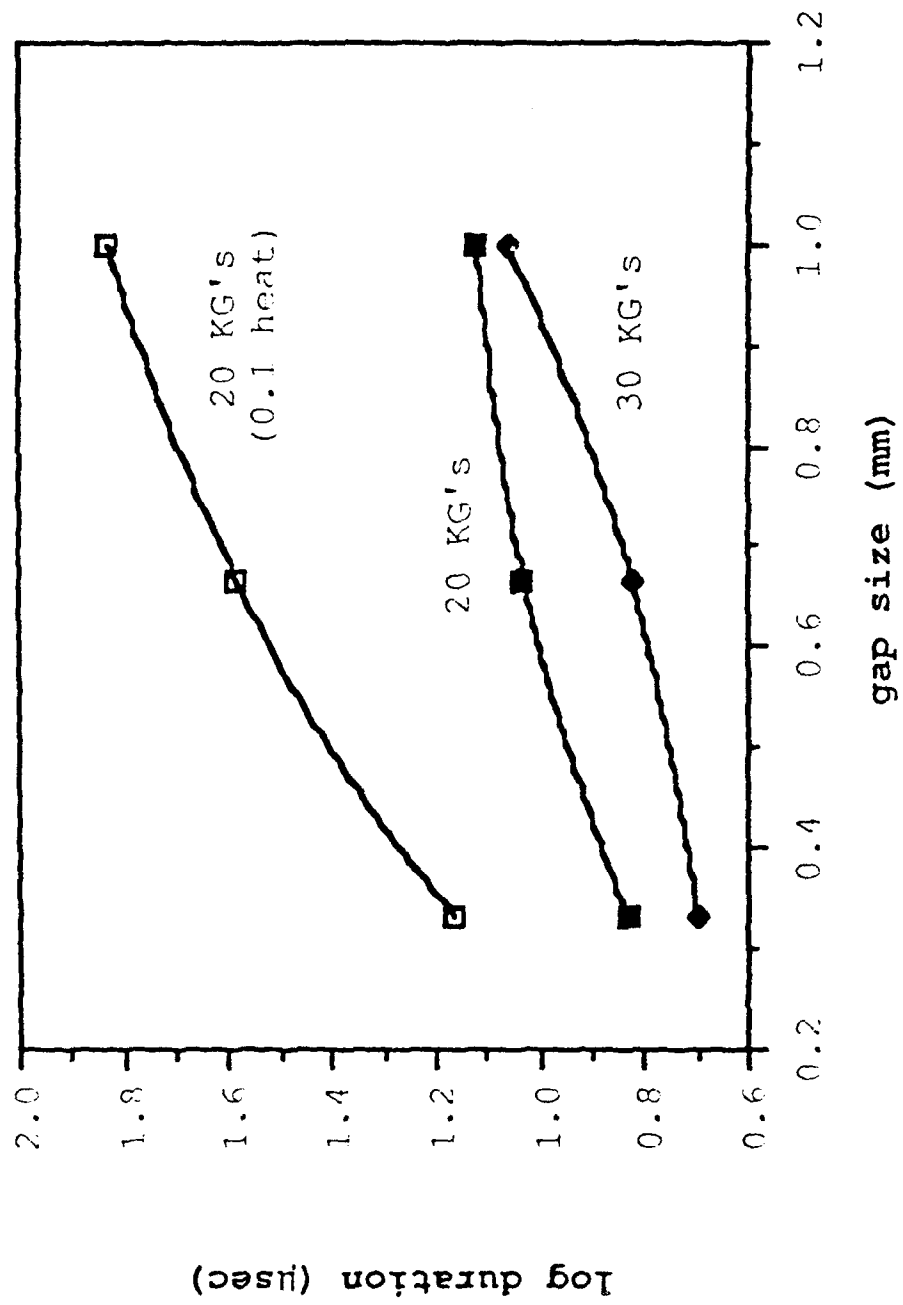
Figure 6. Launch pulse durations at half height

16
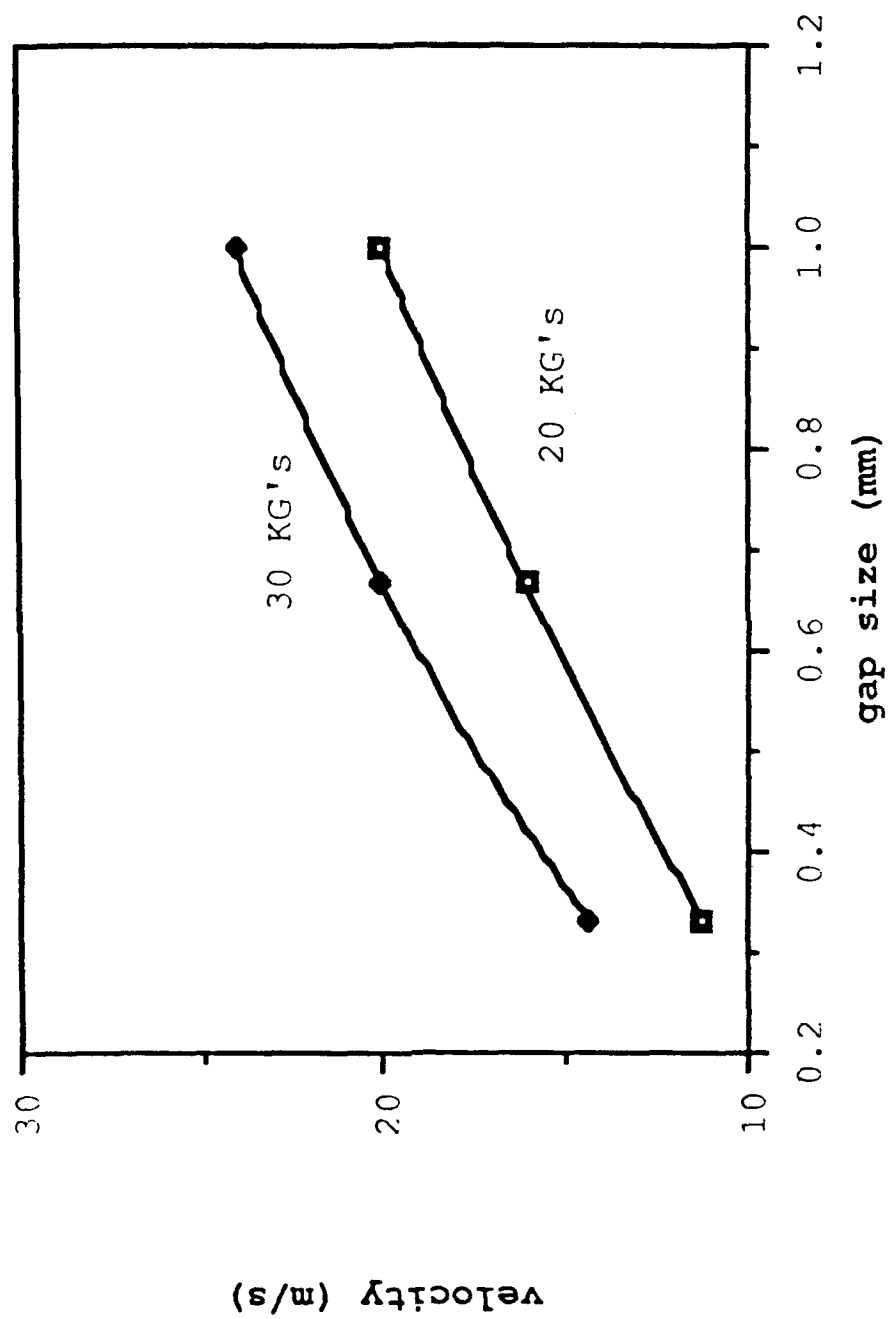
Figure 7. Closing velocity

17
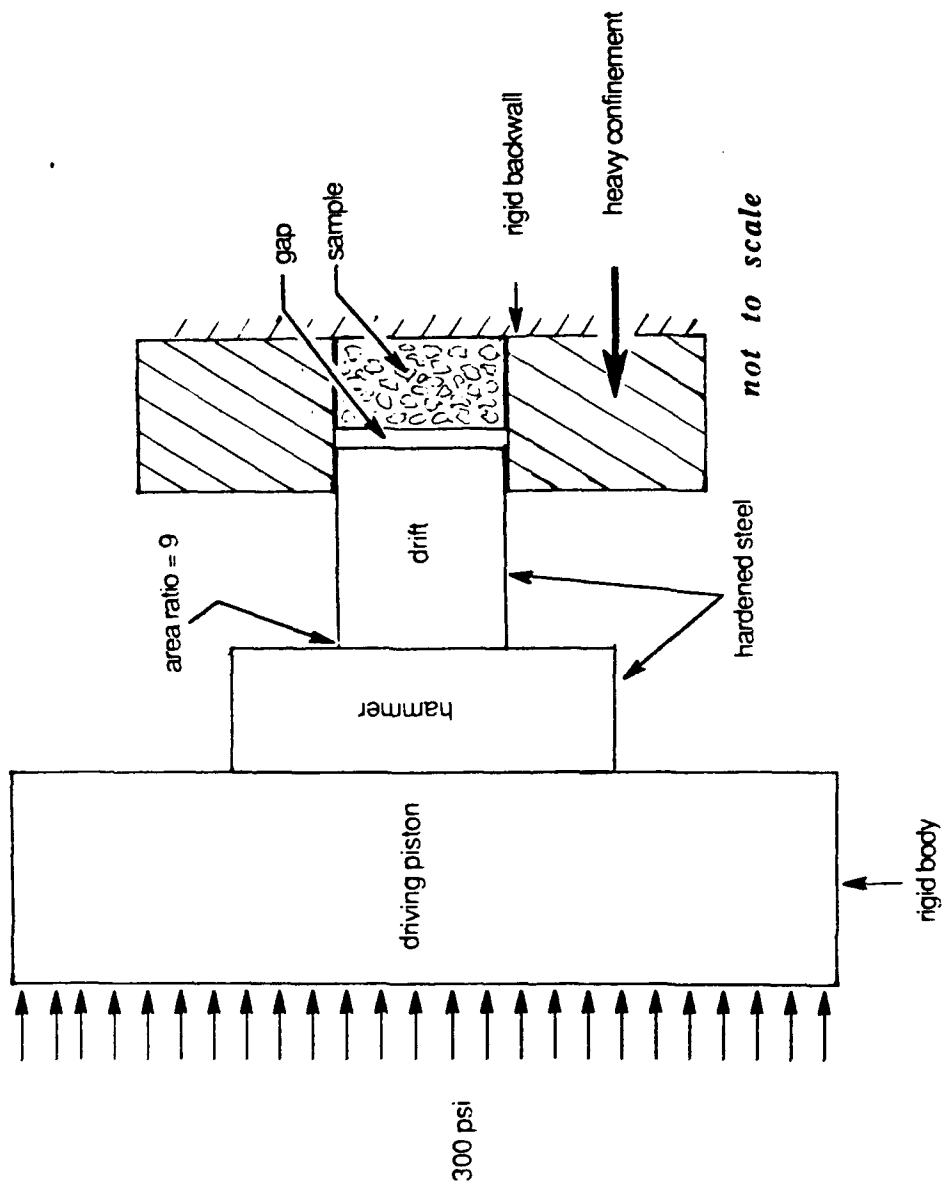
Figure 8.   Picatinny activator

18

9a   PRESSURE HISTORY AT CYCLE *****

9b   VELOCITY HISTORY FOR CYCLE *****

9c   POSITION HISTORY FOR CYCLE *****
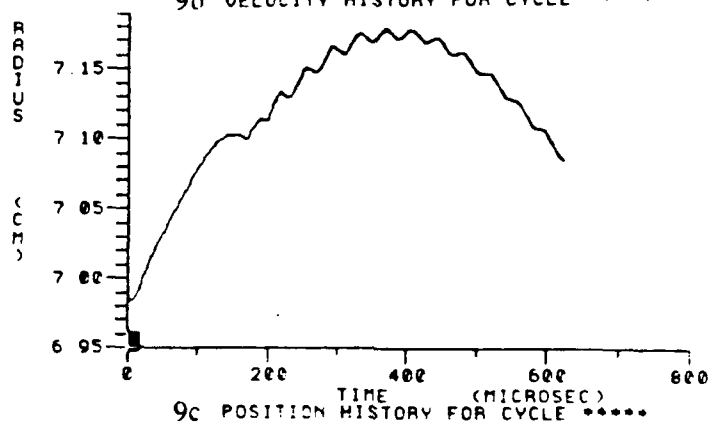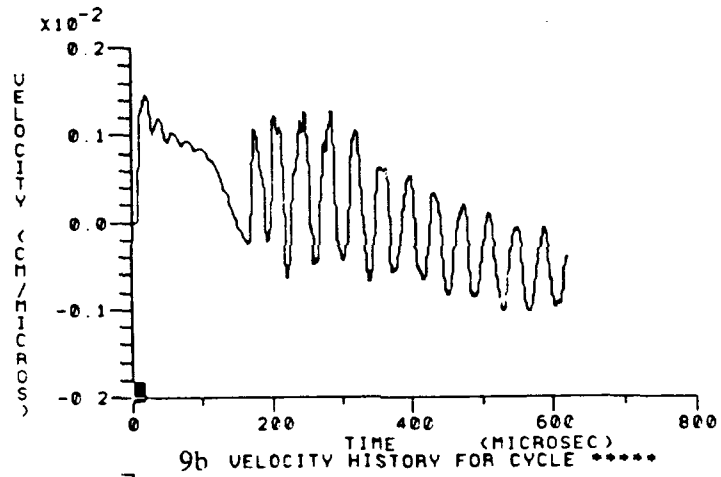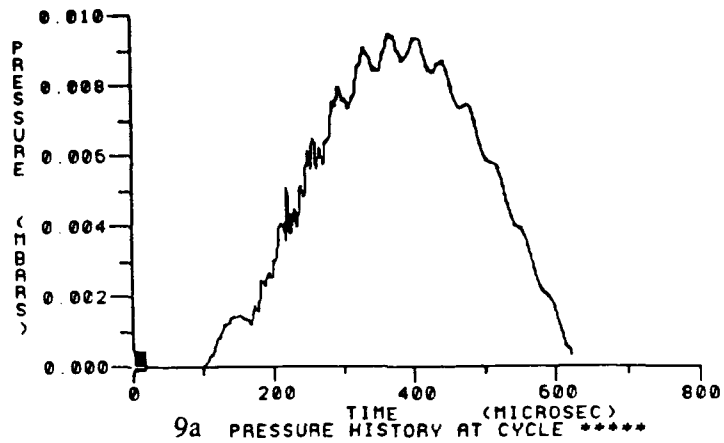
Figure 9.   Activator at 7 M/S

19

9d TEMPERATURE HISTORY FOR CYCLE *****

9e POSITION HISTORY FOR CYCLE *****

9f PRESSURE HISTORY AT CYCLE *****
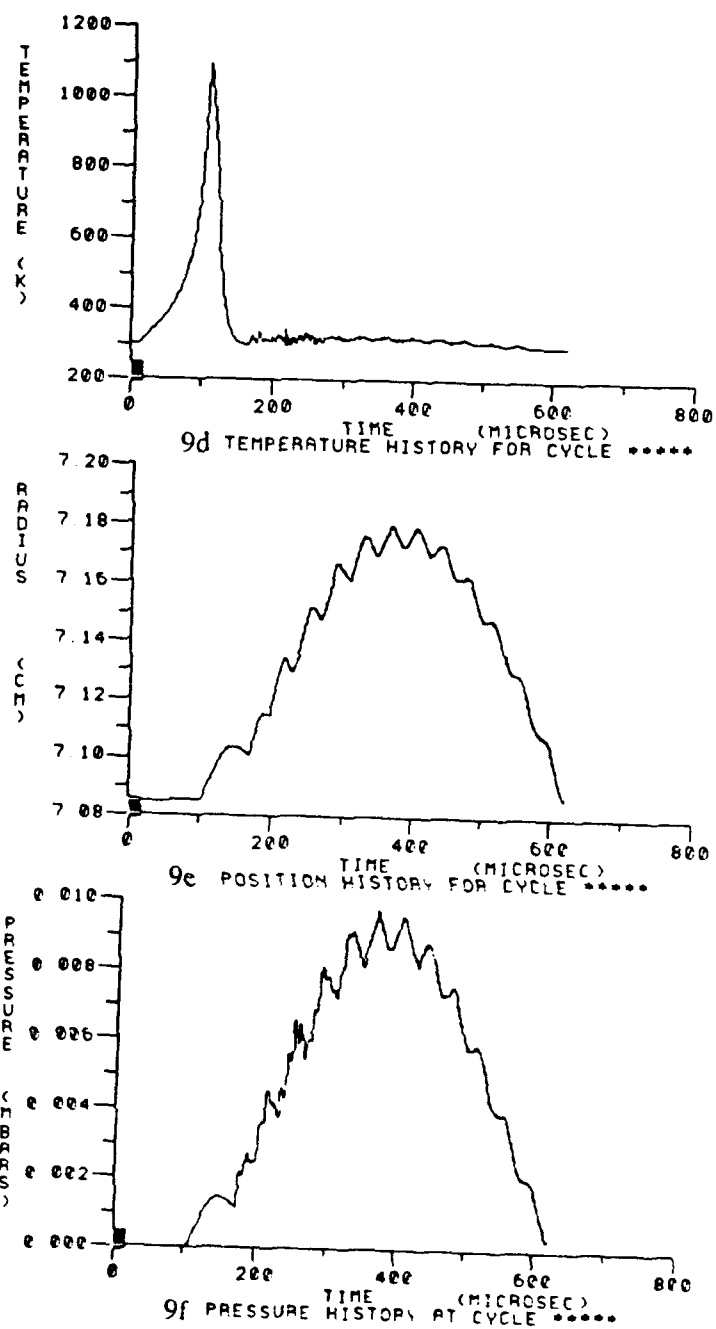
Figure 9. (Continued)

20
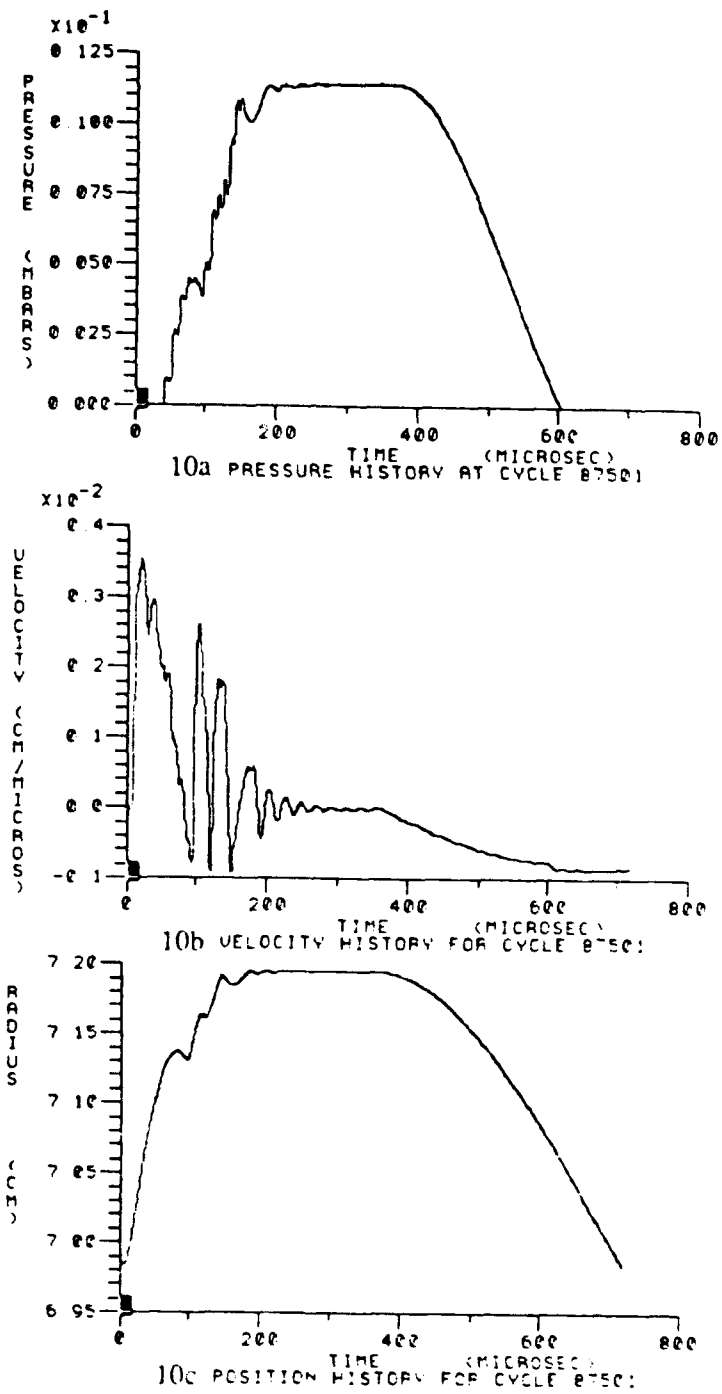
Figure 10. Activator at 17 M/S

21

10d TEMPERATURE HISTORY FOR CYCLE 87501

10e POSITION HISTORY FOR CYCLE 87501

10f PRESSURE HISTORY AT CYCLE 87501
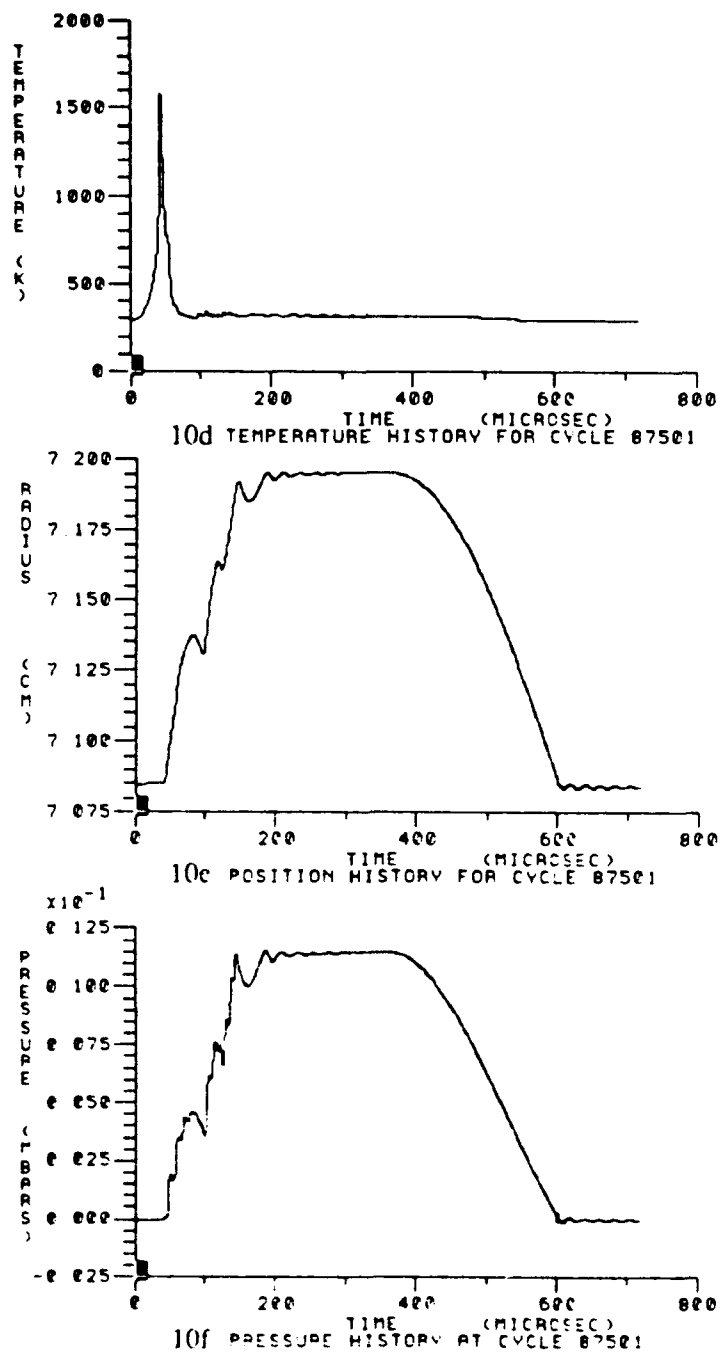
Figure 10. (Continued)

22
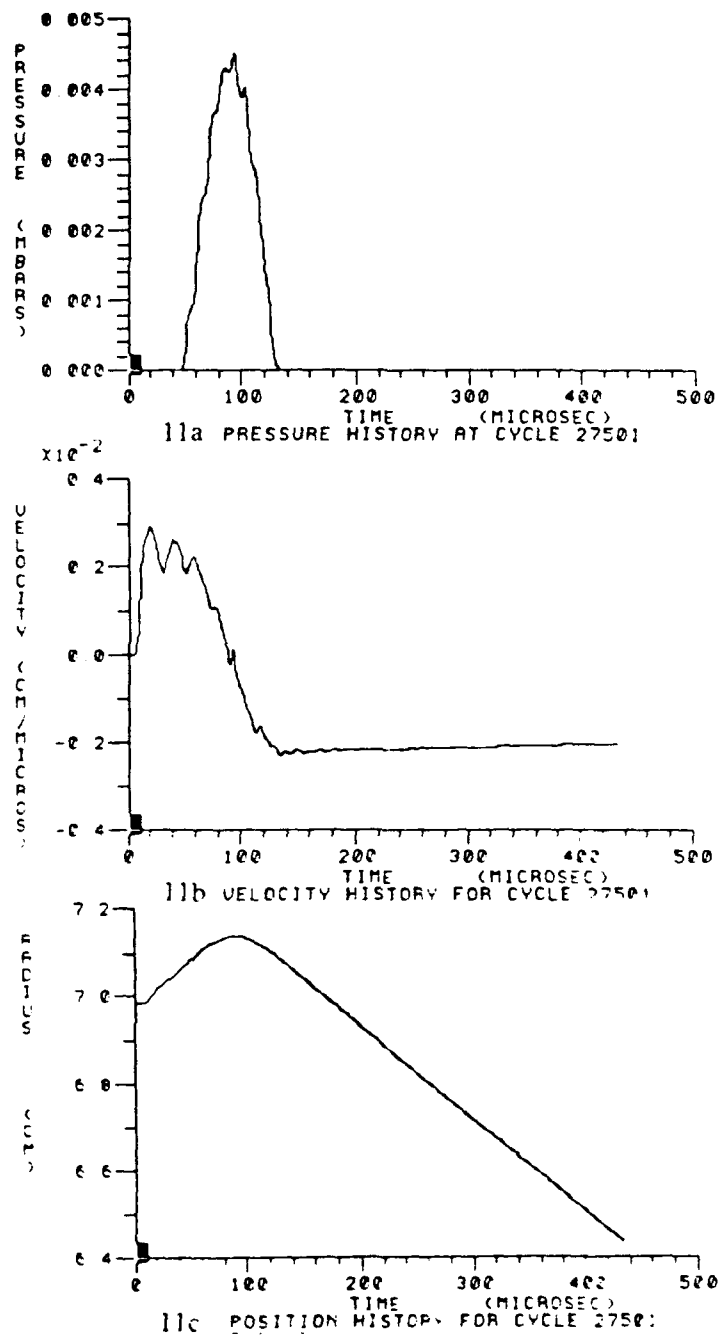
Figure 11. Activator with hammer stop

23

11d  TEMPERATURE HISTORY FOR CYCLE 27501

11e  POSITION HISTORY FOR CYCLE 27501

11f  PRESSURE HISTORY AT CYCLE 27501

Figure 11.  (Continued)

24

12a PRESSURE HISTORY AT CYCLE 11001

12b VELOCITY HISTORY FOR CYCLE 35001

12c POSITION HISTORY FOR CYCLE 35001
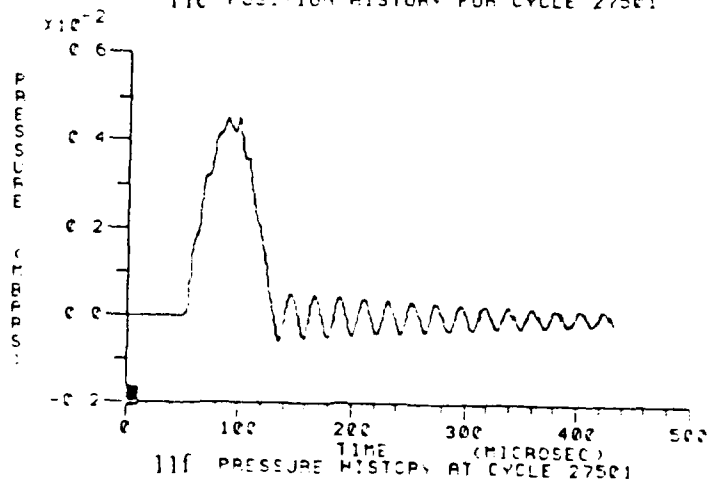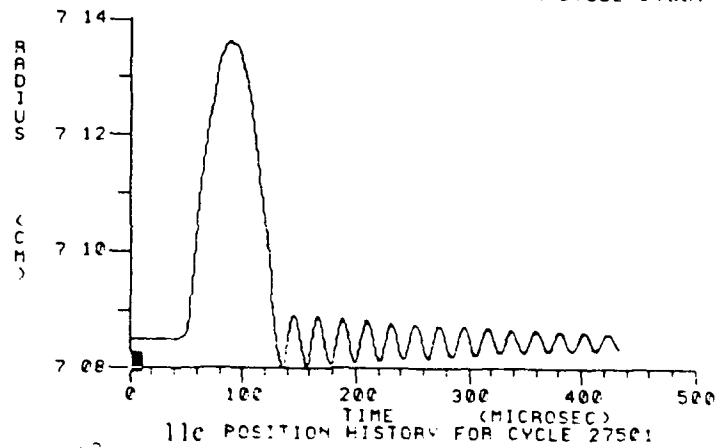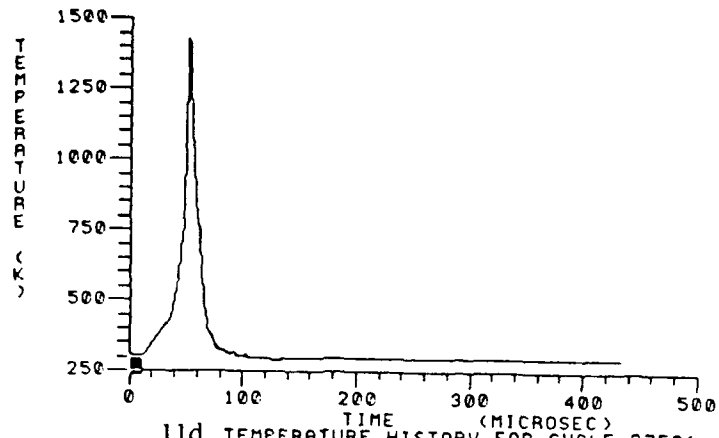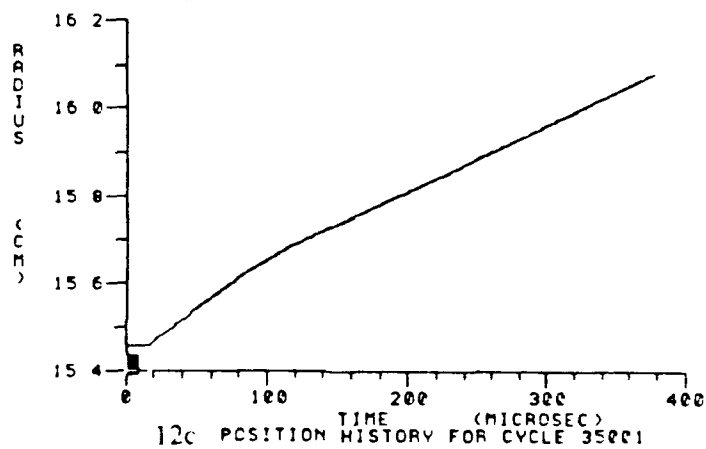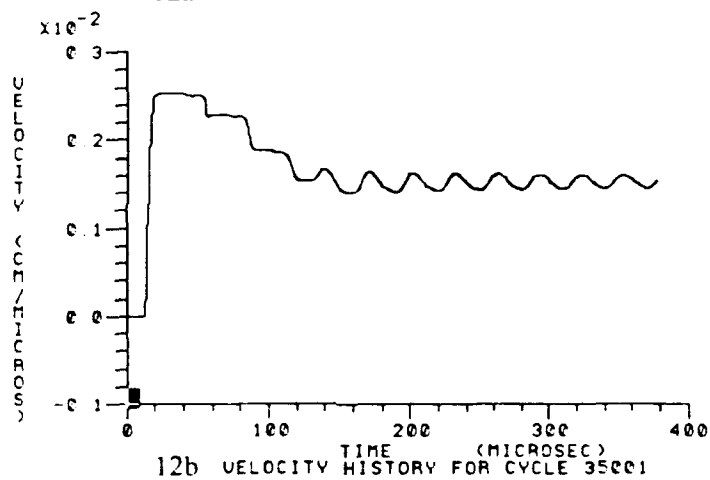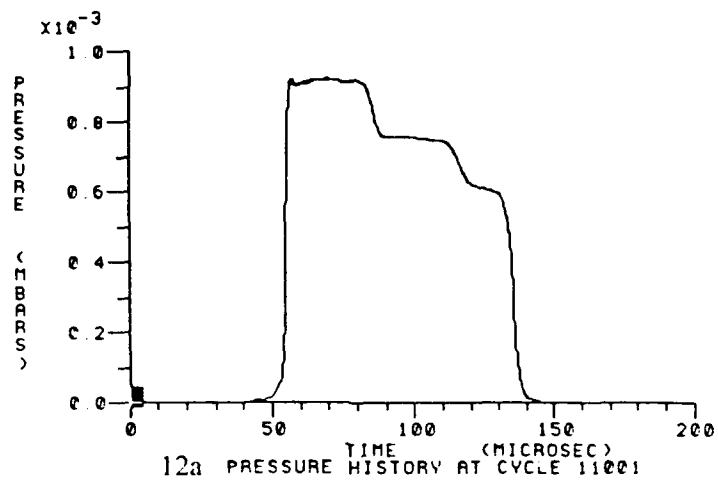
Figure 12. Modified activator

12d TEMPERATURE HISTORY FOR CYCLE 11001
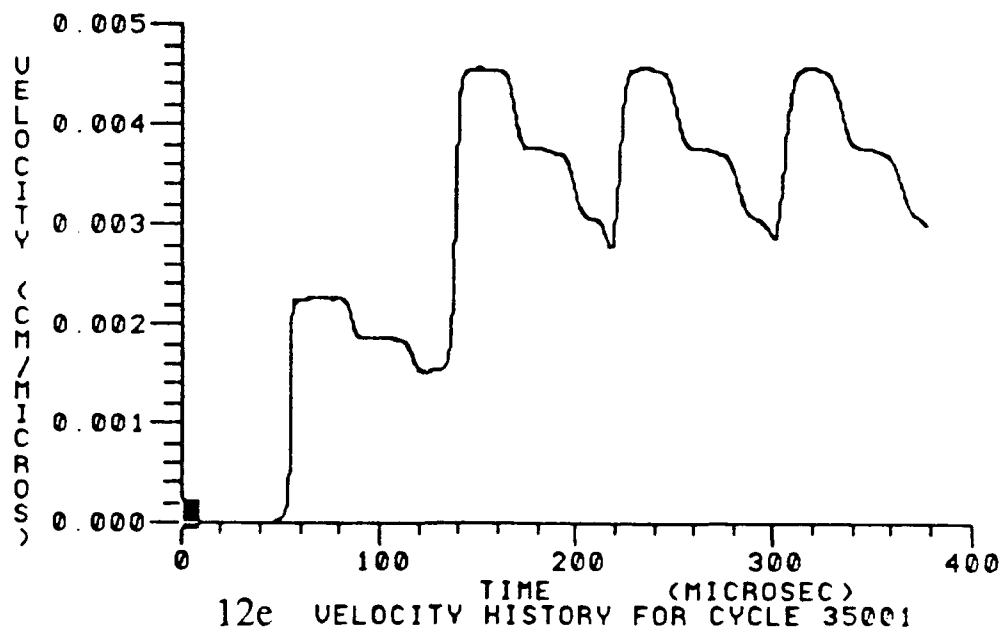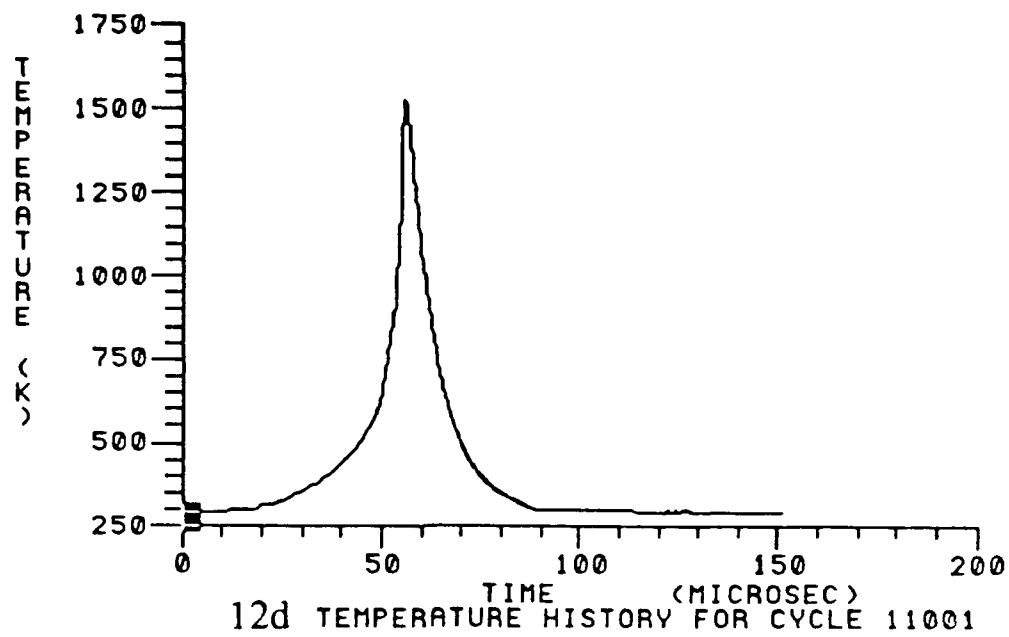


12e VELOCITY HISTORY FOR CYCLE 35001

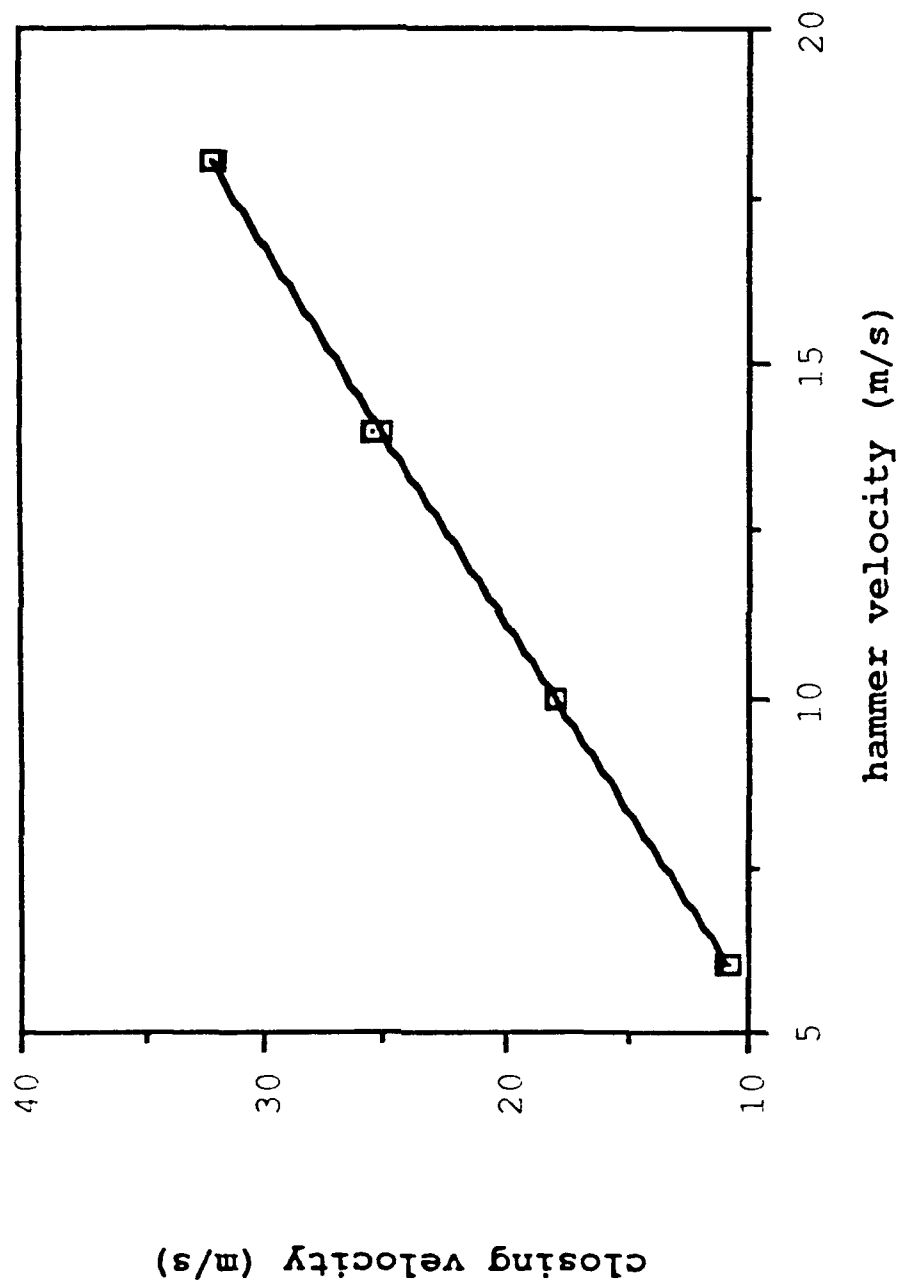Figure 12. (Continued)

26

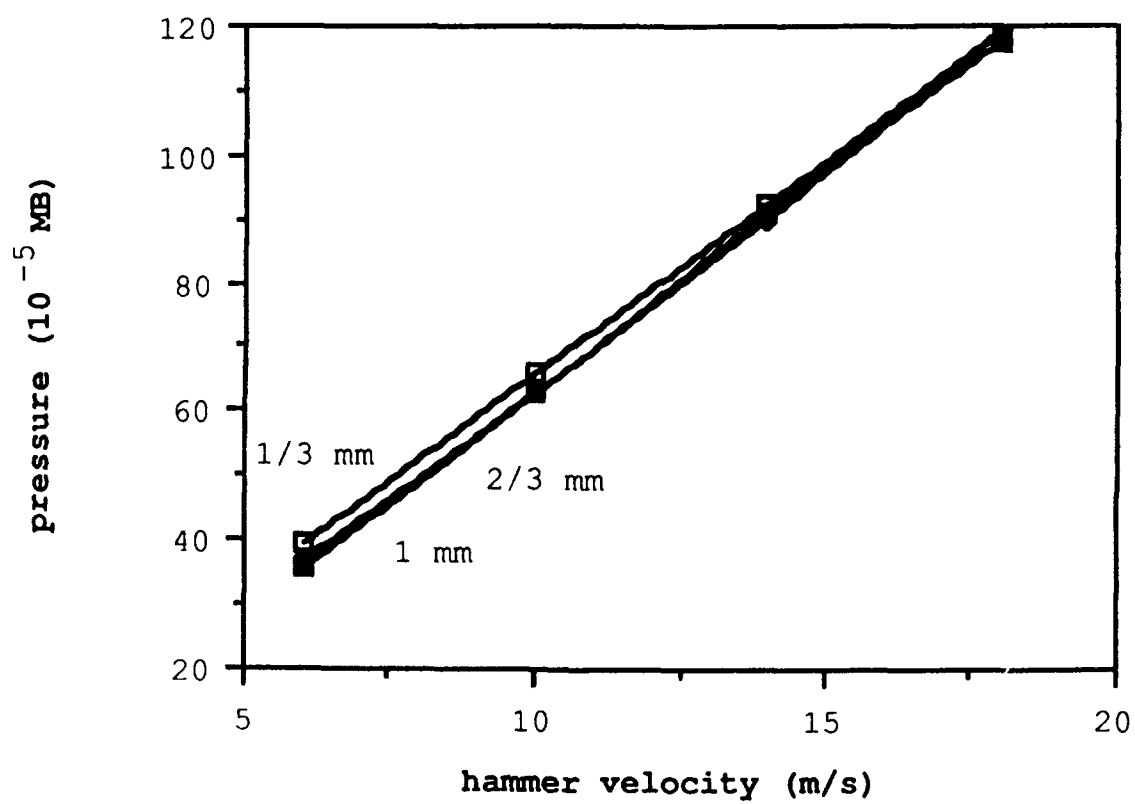Figure 13. Hammer velocity versus gap closing velocity
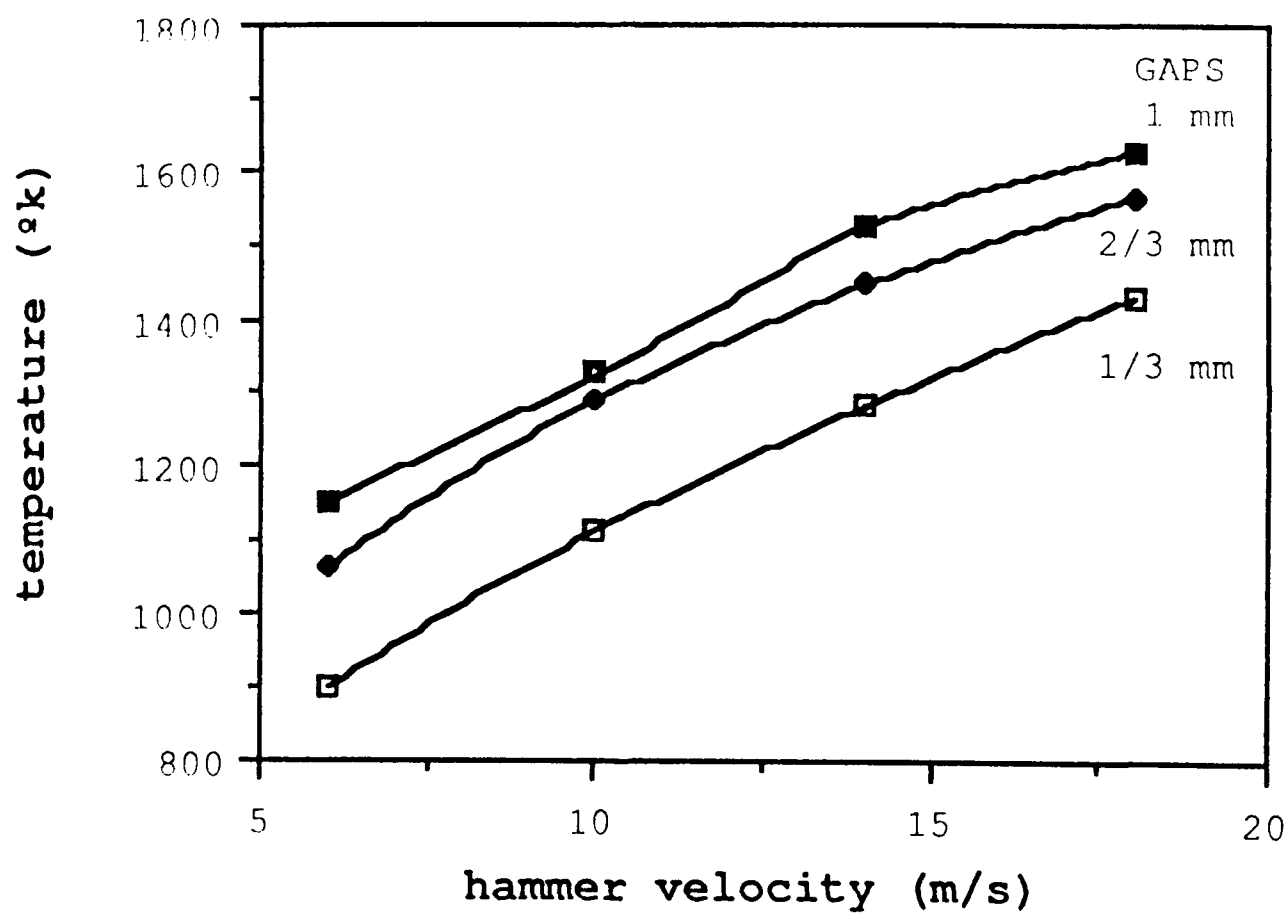
Figure 14. Peak air pressures
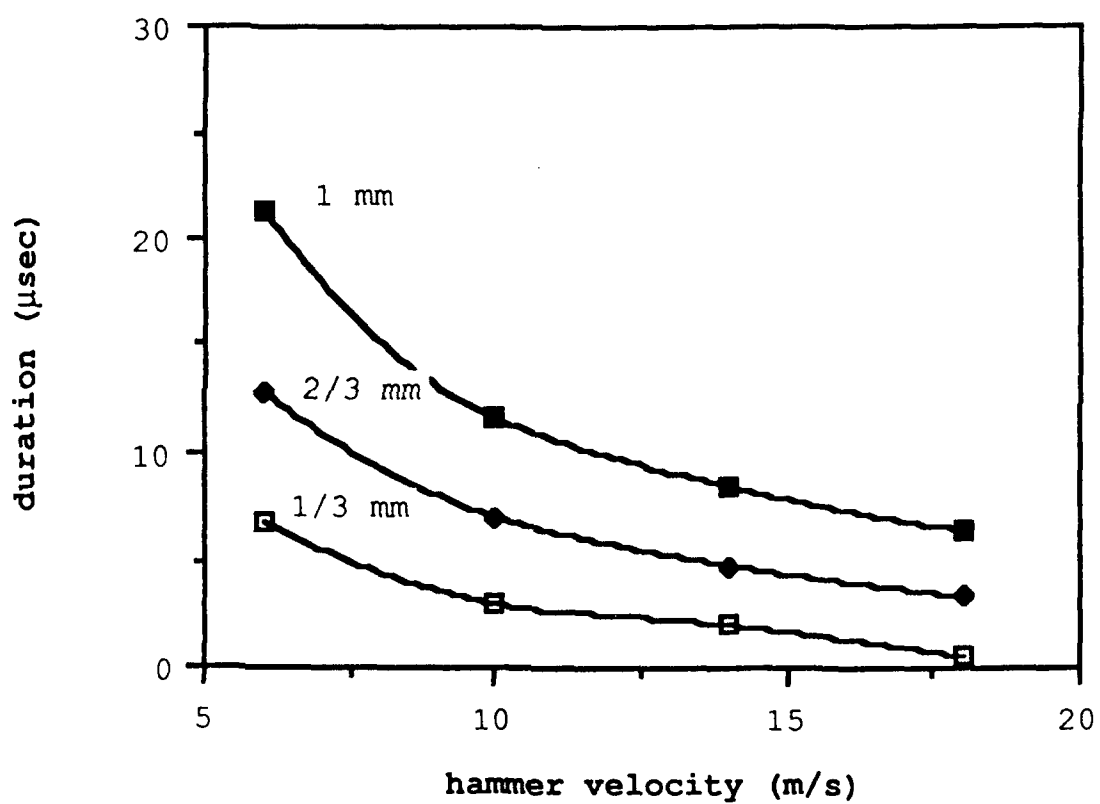
28

Figure 15.  Peak air temperatures

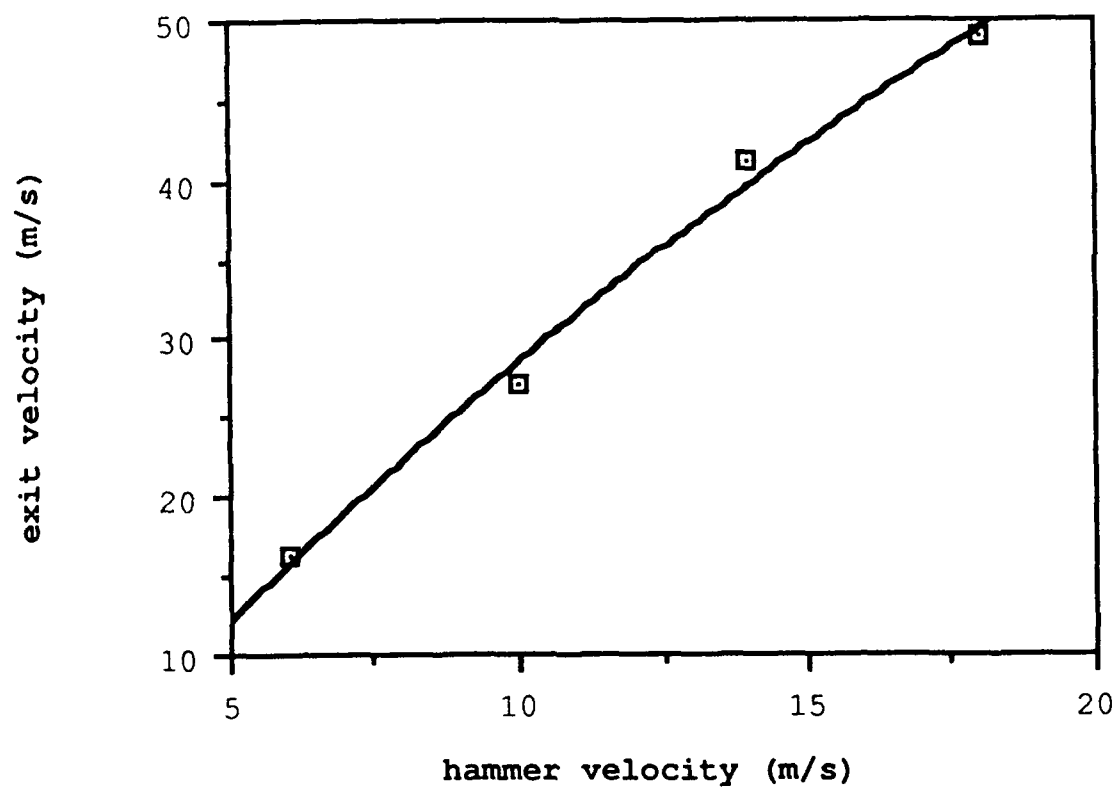Figure 16. Pulse durations at half height

Figure 17. Sample exit velocity

# REFERENCES

1.  Bélanger, C. "Study of Explosive Shell Fillings with Defects in Simulated Gun Launch Conditions," The Ninth Symposium (International) on Detonation, Portland, Oregon, August 28-September 1, 1989.

2.  Schaefer, Siegfried, "High Stress/Rapid Deformation Test - Method and Results -,"DEA 1218 Meeting, Test Center Meppen, June 18-20, 1986.

3.  DeVost, V.F. and Coffey, C.S., "The Premature Susceptibility of Defective MainCharge Loads," NSWC TR 81249, Nov. 1981.

4.  Taylor, B.C., Starkenberg, J., and Ervin, L.H., "An Experimental Investigation of Composition B Ignition Under Artillery Setback Conditions," Ballistic Research Laboratory Technical Report, ARBRL-TR-02276, Dec 1980.

5.  Heinemann, Robert W., and Schimmel, Robert T., "Sensitivity of Explosives to Setback Pressure," Feltman Research and Engineering Laboratories, Picatinny Arsenal, Technical Report 2572, Dec 1958.

6.  Mader, Charles L. and Shaw, Milton Samuel, "User's Manual for Sin, Los Alamos Scientific Laboratory Report LA-7264-M, Sept. 1978.

7.  Pasman,. H.J., "Shell Prematures by Compression Ignition and Their Laboratory Simulation," Defense Research Establishment Valcartier Report, DREV R 707/75, April 1975.

# DISTRIBUTION LIST

Commander
Armament Research, Development and
 Engineering Center
US Army Armament, Munitions and Chemical Command
ATTN: SMCAR-IMI-I (5)
       SMCAR-CO
       SMCAR-TD
       SMCAR-SF
       SMCAR-AEE (3)
       SMCAR-AEE-W (3)
       SMCAR-AEF-C, R.A. Chevalaz
       SMCAR-AEE-WW, B. Fishburn (5)
       SMSMC-QAR-I(D), A. Ko
       SMCAR-FSP-I, P. Burke
       SMSMC-DSM-AA (D), F. Sedlacek
Picatinny Arsenal, NJ 07806-5000


Commander
U.S. Army Armament, Munitions and Chemical Command
ATTN: AMSMC-GCL(D)
Picatinny Arsenal, NJ 07806-5000


Administrator
Defense Technical Information Center
ATTN: Accessions Division (12)
Cameron Station
Alexandria, VA 22304-6145


Director
U.S. Army Materiel Systems Analysis Activity
ATTN: AMXSY-MP
Aberdeen Proving Ground, MD 21005-5066


Commander
Chemical Research, Development and Engineering Center
U.S. Army Armament, Munitions and Chemical Command
ATTN: SMCCR-MSI
Aberdeen Proving Ground, MD 21010-5423

Commander
Chemical Research, Development and Engineering Center
U.S. Army Armament, Munitions and Chemical Command
ATTN: SMCCR-RSP-A
Aberdeen Proving Ground, MD 21010-5423

Director
US Army Ballistic Research Laboratory
ATTN: AMXBR-OD-ST
SLCAR-TB-EE, R. Frey (2)
                J. Starkenberg
Aberdeen Proving Ground, MD 21005-5066

Commander
U.S. Army Armament, Munitions and Chemical Command
ATTN: SMCAR-CCB-TL
AMSMC-DS
Rock Island, IL 61299-6000

Commander
U.S. Army Armament, Munitions and Chemical Command
ATTN: SMCRI-TL/Technical Library
Rock Island, IL 61299-5000

Director
US Army TRADOC Systems Analysis Activity
ATTN: ATTA-SL
White Sands Missile Range, NM 88002

Commander
Watervliet Arsenal
Benet Laboratories, Bldg. 40
ATTN: SMCAR-CCB-DI
Watervliet, NY 12189-5000

Conrad Bélanger
Defence Research Establishment Valcartier
2459, Pie XI Blvd., North (P.O. Box 8800)
Courcelette, Quebec, GOA 1RO, Canada

Dr. D. Pillasch
Aerojet Corp.
1100 W. Hollyvale (P.O. Box 296)
Bldg. 57, Dept. 2711
Azusa, CA 91702

Robert Tompkins
Aliant Techsystems
MN 38-3300
10400 Yellow Circle Dr.
Minnetonka, MN  55343